ACS APPLIED MATERIALS & INTERFACES

Research Article

Cite This: ACS Appl. Mater. Interfaces 2019, 11, 17147−17156

www.acsami.org

Supramolecular Microgels with Molecular Beacons at the Interface for Ultrasensitive, Amplification-Free, and SNP-Selective miRNA Fluorescence Detection

Tania M. Caputo,[†] Edmondo Battista,[†,‡] Paolo A. Netti,[†,‡,§] and Filippo Causa*[,†,‡,§]

[†]Center for Advanced Biomaterials for Healthcare@CRIB, Istituto Italiano di Tecnologia (IIT), Largo Barsanti e Matteucci 53, 80125 Naples, Italy

[‡]InterdisciplinaryResearch Centre on Biomaterials (CRIB), Università degli Studi di Napoli "Federico II", Piazzale Tecchio 80, 80125 Naples, Italy

[§]Dipartimento di Ingegneria Chimica del Materiali e della Produzione Industriale (DICMAPI), University "Federico II", Piazzale Tecchio 80, 80125 Naples, Italy

Supporting Information

ABSTRACT: In this study, a supramolecular structure with femtomolar biorecognition properties is proposed for use in analytical devices. It is obtained by an innovative interface between synthetic hydrogel polymers and molecular beacon (mb) probes. Supramolecularly structured microgels are synthetized with a core−shell architecture with specific dyes polymerized in a desired compartment. Mb probes are opportunely conjugated at the microgel interface so that their recognition mechanism is preserved and their spatial distribution is optimized to avoid crowding effects. The miR-21, a microRNA involved in various biological processes and usually used as a biomarker in early cancer diagnosis, has been selected as the target. The results demonstrate that by tuning the spatial distribution of molecular probes immobilized on the microgel and/or the amount of microgels, the assay shows scalable sensitivity reaching a limit of detection down to about 10 fM, without amplification steps and with detection time as short as 1 h. The assay results specific toward single mutated targets, and it is stable in the presence of high-interfering oligonucleotides concentrations. The miRNA target is also detected in human serum with performances similar to those observed in PBS buffer because of microgel antifouling properties without the need of any surface treatment. All tests were performed in a low sample volume (20 μL). As a result, mb-microgel represents an innovative biosensor to precisely quantify microRNAs in a direct (mix&read), scalable, and selective way. Such an approach paves the way for creating innovative biosensing interfaces with other probes, such as hairpins, aptamers, and PNA.

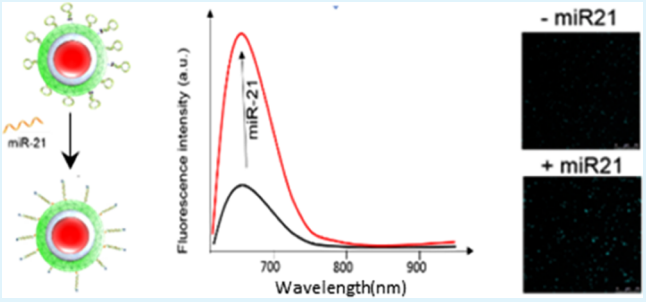

KEYWORDS: *molecular beacons, hydrogel interface, bead fluorescence sensor, mix&read assay, microRNA*

INTRODUCTION

Molecular beacons (mb) are widely used as oligonucleotide probes because of the higher thermodynamic stability of the hairpin structure, efficient signal switching, and the numerous reporter dyes available.[1−4] Furthermore, with respect to other oligonucleotide probes, mb show many advantages, including faster kinetics of hybridization, excellent sensitivity, selectivity, and real-time detection capability.[5] Because of its hairpin-stem unimolecular reaction, mb are capable of differentiating between two target sequences that differ by as little as a single nucleotide.[6,7] Their intrinsic properties have made mb extensively employed free in solution or immobilized on solid substrates.

Solid surfaces have been largely functionalized with mb for biosensing applications obtaining efficient results in terms of specificity and sensitivity.[8−15] As a result, high-throughput analysis and parallel screening of several molecules of interest are achieved, reducing both the assay time and cost. However, when mb are immobilized on solid surfaces, the fluorescence background usually increases because of nonspecific oligonucleotide−surface interactions and crowding effects among the immobilized oligonucleotide probes.[16] This negatively affects both the hybridization ratio and the assay sensitivity. In the case of glass substrates, spacing linkers, such as poly(thymidine/adenosine) (poly (T/A poly)) and poly(ethylene glycol) (PEG),[14,17] have been introduced to distance the mb from the surface. Alternatively, surface polymer coating[18] and nucleic acid analogues[19] have been used to increase the mb stability. Such modifications decrease the surface effect and slightly improve the mb performance. Gold surfaces also

Received: December 28, 2018
Accepted: April 25, 2019
Published: April 25, 2019

DOI: 10.1021/acsami.8b22635
ACS Appl. Mater. Interfaces 2019, 11, 17147−17156

represent a valid substrate to immobilize quencher-free mb by standard gold−thiol chemistry. These functionalized substrates achieve nanomolar sensitivity and high specificity.[20] Nevertheless, nonspecific adhesion and non-uniform distribution of mb on the gold surface can reduce the biosensing performance. mb have been also immobilized on substrate as graphene,[21−24] which works as a super-quencher with a long-range nanoscale energy transfer property. As a result, when mb are immobilized on graphene oxide substrates, the fluorescence background strongly decreases and the signal-to-noise ratio (hence the sensitivity) increases. These biosensors show single nucleotide polymorphism (SNP) selectivity and low sensitivity (in nanomolar to picomolar order) that usually require the combination with amplification methods.[25] However, for each substrate, nonspecific adsorption occurring in biological fluids largely impairs direct and easy detection of target oligonucleotides, whereas the kinetics is usually depressed after immobilization on solid surface.[26]

The use of mb on polymeric microparticles has a long story.[27] However, they suffer from the need of passivation or surface treatment to work in biological fluids and for poor stability of emitting molecules adsorbed for the optical barcoding. On the contrary, polymeric microgels or other hydrogel particles possess ideal and superior features for biosensing applications. Hydrogels are three-dimensional hydrophilic materials endowed with tunable chemical and physical nature.[28] The versatility of these materials has gained popularity in many biomedical applications, such as drug delivery, tissue engineering, and biosensors.[29,30] Regarding biosensing, hydrogels can be functionalized with several biorecognition elements and possess solution-like property capable of improving the sensitivity and reducing the detection time.[31] In particular, hydrogel microposts,[32] arrays,[33] pads,[34] and microspheres[35] are being developed for biosensing applications. Indeed, the hydrogel solution-like property enhances both the thermodynamic association constants[36] and the kinetics (association rate k_{on})[37] for oligonucleotides and other biomolecules. The antifouling property imparts selectivity in biological fluids,[38] allowing direct measurement with high specificity without any treatment of the surface. Indeed, when mb are conjugated on hydrogel surfaces, the high-fluorescence background can be reduced.[39]

Furthermore, hydrogel microparticles offer a suitable substrate for biosensing.[40−43] Indeed, by means of their chemical flexibility, it is easy to stably encode spectral signature ensuring a potentially wide range of possible barcodes. As a result, microgels with core−shell architecture or barcoded hydrogel particles are capable of scalable,[44] sensitive, and multiplex optical detection.[45] Their particle nature[46] allows for assay versatility, multiplex assay,[40,47] easy manipulation in assay steps, and fast analysis in flow,[48] also compatible with cytometers.[49]

Therefore, the combination of well-known mb with microgels or hydrogel particles could represent a very promising new interface, combining the performance of high specificity of mb with antifouling properties and high chemical structure flexibility of microgels. However, the development-sensing interfaces represented by mb on the hydrogel interface do not represent a trivial implementation because a number of technical questions have to be addressed in order to be successful in its integration. First, the bioconjugation of mb on hydrogel occurs at a highly hydrated and flexible interface rather than on a solid surface. This opens up important questions on whether the molecular switch between the folded (turn off) and unfolded conformation (turn on) of mb is guaranteed by the tether nature and length as well as by spatial distribution of mb bioconjugated on microgels. These questions are addressed in the present paper in order to design a new interface for biosensing applications with the capability to reduce unspecific interactions without the need for any surface treatment or passivation.

MicroRNA (or miRNA) are non-coding RNA sequence of about 22−25 nt.[50] MiRNA aberrations can be correlated with specific pathological states, such as cancer,[51] cardiovascular diseases,[52] neurological disorders,[53] or infections.[54] Circulating miRNAs are often used as biomarkers for the early diagnosis, prognosis, and follow-up of several pathological conditions.[52] Traditional methods to detect miRNA are mainly based on amplification methods and in situ hybridization.[55,56] However, despite all the techniques developed, miRNA detection is still challenging because of the small size, the sequence similarity, the low abundance, the intra- and inter-variability, the complexation within vesicles and lipids, and the presence of interfering molecules in biological fluids.[57] For this reason, although miRNAs have widely proved to be suitable biomarkers, their application in clinical practice is still limited, and the development of innovative methods for their detection is still required.

Here, we present biosensing microgels, made up of supramolecular structure of PEG, endowed with mb at interface, capable of detecting microRNAs. Such approach enlarges the spectrum of biosensing applications of mb by improving their sensitivity (compared to solution) and by allowing in-serum direct detection. The hsa-miR-21, an miRNA involved in various biological processes[58,59] and usually used as a biomarker in early cancer diagnosis, has been selected as the target.

This work investigates the potential of mb-microgels, assessing the question of how the probe structure and spatial distribution at the microgel interface affect the sensitivity and specificity of the detection. This could combine the well-assessed advantages of mb with the capability of microgels to improve sensitivity and allow mix&read assay. Our results demonstrate that mb-microgels achieve femtomolar sensitivity in miR-21 detection, avoiding preliminary amplification steps, also in serum. Moreover, functionalized microgels are capable of SNP discrimination and reduced time of analysis. Such approach could also permit large multiplex ability by dye polymerization in polymer network.

EXPERIMENTAL SECTION

Materials. Poly(ethylene glycol) dimethacrylate average Mn 550 (PEGDMA), acrylic acid (AAc), potassium persulfate (KPS), fluoresceine *O*-methacrylate, 1-ethyl-3-(3-dimethylaminopropyl) carbodiimide (EDC), polyvinyl alcohol (PVA) 40−88, dimethyl sulfoxide, sodium hydroxide, 4-morpholineethanesulfonic acid sodium salt (MES), and biological-grade water were all purchased from Sigma-Aldrich and used as received. The dye methacryloxyethylthiocarbonyl-rhodamine B was obtained from Polyscience Inc. Phosphate buffered saline tablets were supplied by MP biomedicals. DNA and RNA oligonucleotides were purchased from Metabion International with HPLC purification.

mb Design. Two mb complementary to the miR-21 were designed. The mb contained a fixed loop complementary to the target made of 22 bases and a stem of 5 or 6 bases (MBS5 or MBS6). The 5′ terminus was modified with an ATTO647N fluorophore and a 12-carbon amino spacer, whereas a BlackBerry Quencher 650 (BBQ-

DOI: 10.1021/acsami.8b22635
ACS Appl. Mater. Interfaces 2019, 11, 17147−17156

Table 1. mbs and Target Sequences Tested[a]

	sequence (5′−3′)	length (nt)
MBS5	**CGCGC***TCAACATCAGTCTGATAAGCTA***GCGCG**	32
MBS6	**CGCGCG**TCAACATCAGTCTGATAAGCTA**CGCGCG**	34
miR-21	UAGCUUAUCAGACUGAUGUUGA	22
miR-21-1a	UA**U**CUUAUCAGACUGAUGUUGA	22
miR-21-1b	UAGCUUAUCA**A**ACUGAUGUUGA	22
miR-21-2	UA**U**CUUAUCA**A**ACUGAUGUUGA	22
miR-21-3	UA**U**CUUAUCA**A**ACUGAUGUU**A**A	22
non-matching (miR-143-3p)	UGAGAUGAAGCACUGUAGCUC	21

[a]The nucleotides of the loop are in italics, whereas those of the stem are in bold underline. The mutations introduced in the sequences are in bold.

650) was added on the 3′ terminus. Both mb were suspended in nuclease-free water to a concentration of 100 μM and stored at −20 °C.

To assess the specificity of mb, non-matching sequence (miR-143) and three mutants of the wild-type miR-21 were also used in the hybridization assays. Specifically, for the miR-21 mutants, 1, 2, or 3 nucleotides of the sequence were mutated: miR-21-1a had one nucleotide mutated at the end of the loop, near the stem; miR-21-1b had one mutated nucleotide in the center of the loop; miR-21-2 had both mutated nucleotides in the center and at the end of the loop; miR-21-3 had three mutated nucleotides (Table1).

The kinetics of hybridization in the presence of the wild-type miR21, the mutated miR-21 sequences, and a non-matching miR were measured by mixing 500 nM of the sequences to 50 nM of mb in 500 μL of PBS buffer. The fluorescence recovery as a function of time was recorded by a spectrofluorometer. Fluorescence spectra were collected in a 1 cm path length cuvette with a HORIBA JobinYvon model FluoroMax-4 spectrofluorometer equipped with a Peltier temperature controller. The sample was excited at 647 nm with a slit width of 5 nm, and emission spectra were collected from 667 to 750 nm with a slit width of 5 nm.

Melting curves for both mb alone and in the presence of the miRNA sequences were generated to identify their melting temperatures. Melting curves were obtained by monitoring the fluorescence intensity as a function of temperature. In particular, 500 μL of PBS buffer solution containing 50 nM of mb alone or mixed with 500 nM of miRNA was initially denatured (3 min 95 °C), and then the temperature was decreased from 95 to 20 °C, with a scan rate of 1 °C/2 min. Fluorescence spectra were measured as reported above, exciting the sample at 647 nm and collecting the emission intensity from 667 to 750 nm.

Microgel Synthesis. Microgels with a multi-shell architecture were synthetized through a multistep synthesis, as previously described.[40] Briefly, core nanoparticles made of PEGDMA 1% (w/v) and rhodamine B acrylate monomer (0.1 mM) were synthetized via free-radical precipitation polymerization. KPS (2.2 mM) in PVA 1% (w/v) was used as an initiator, heating to 65 °C for 7 h in N_2 atmosphere. Nanoparticles were dialyzed for 15 days, purified several times by centrifugation (for 15 min at 6500 rpm), and worked as a seed for the subsequent two-shell polymerization. The first shell was obtained using PEGDMA 0.5% (w/v), PVA 0.5% (w/v), and KPS (1.1 mM), heating to 65 °C for 6 h in N_2 atmosphere. The microgels were dialyzed and purified several times by centrifugation (15 min at 9000 rpm). The second shell was obtained by adding to the aqueous suspension of core/1st shell microgels PEGDMA 0.5% (w/v), KPS (1.1 mM), AAc 0.25% (w/v), and fluorescein *O*-methacrylate (0.1 mM). The reaction was allowed to proceed for 6 h. The microgels were dialyzed for 15 days, purified several times by centrifugation (for 15 min at 6500 rpm), and suspended in deionized water to remove unreacted monomer, oligomers, and surfactants, and then stored at 4 °C prior to use until further use. The microgel size, zeta potential, conductivity, and electrophoretic mobility were characterized by dynamic light scattering (Malvern Zetasizer Nano ZS instrument, 633 nm laser, 173° scattering angle). The carboxyl group content was quantified by titration before further conjugation of the mb.

mb Conjugation. Bioconjugation was optimized by coupling 1, 0.5, and 0.1 nmol of mb. Before the reaction, 1 mg of microgel was incubated in 450 μL MES pH 6, whereas mb were incubated in 50 μL MES pH 6 enriched with 200 mM of NaCl, both for at least 5 h. Then, the carboxylic groups on the microgel were activated using 500 mM of the coupling agent EDC by stirring vigorously for 30 min at 5 °C. Subsequently, the pre-hybridized mb solution was added to the microgels by incubating overnight at room temperature. Mb-microgels were washed 3 times to remove the unreacted mb and suspended in PBS buffer. For each microgel functionalization, the kinetics of hybridization with the miR-21 target was measured through a spectrofluorometer. For this purpose, 20 nM of wild-type miR-21 solution was mixed to 25 μg/mL of mb-microgels in 500 μL of hybridization buffer.

Microgel Assay. The assay was easily performed by mixing the microgels to the sample solution containing the target sequences, without preliminary steps of amplification. Such solution is incubated at room temperature and the fluorescence recovery is measured. In particular, mb-microgels limit of detection (LOD) and limit of quantification (LOQ), scalable sensitivity, kinetics of hybridization, and specificity were measured by confocal laser scanning microscopy (CLSM).

To estimate the LOD and LOQ, 5 μg/mL of each mb-microgel was mixed with 20 μL of samples at different target concentrations, ranging from nM to aM, loaded into a μ-slide 18-well flat (Ibidi, Martinsried, DE) and incubated at room temperature overnight. Moreover, to prove the assay scalability, only in the case of microgels with the lowest functionalization (0.1 nmol), the microgel concentration was decreased down to 0.5 μg/mL.

The kinetics of hybridization were measured by mixing 100 nM and 100 pM of wild-type miR-21 with 5 μg/mL of mb-microgels in a final volume of 20 μL. Fluorescence intensity was collected after 1, 3, 5, and 24 h. The samples were analyzed by CLSM-SP5 with an objective HCX PL APO CS 63 × 1.40 oil (Zeiss), by using Helium neon laser 543 and 633 nm. Power lasers and detector gains were always kept constant, with a section thickness of 3.04 airy unit, scan speed of 8000 Hz, and image size of 144.7 × 144.7 μm^2 (resolution 1024 × 1024). For each target concentration, 3 or more images were collected and more than 500 microgels were analyzed. The images were thresholded by the Otsu algorithm and then processed with the ImageJ Analyze Particles function to computationally determine the number of single fluorescent particles sizing in the range of 1 μm.

Assay Specificity. The assay specificity was tested by adding 5 μg/mL of mb-microgels (with 0.1 nmol functionalization) to 20 μL of buffer solution containing 50 pM of each mutated miR-21 sequence, 50 pM of non-matching miR (miR-143), and 50 pM of 1:1 miR21-1a/miR-143 (Table 1). Moreover, mb-microgels were mixed with 50 pM of wild-type miR-21 containing 50 pM or 5 nM of mir21-1a and 50 pM or 5 nM of 1:1 of miR21-1a/miR-143. The solution was incubated overnight at room temperature, whereas images were collected and analyzed as previously described.

Assay in Complex Fluids. To simulate the detection performance of microgels in a complex fluid, the assay was carried out in human serum by mixing 5 μg/mL of mb-microgels in 20 μL of human serum enriched with 2 pmol of wild-type miR-21. The samples were

DOI: 10.1021/acsami.8b22635
ACS Appl. Mater. Interfaces 2019, 11, 17147−17156

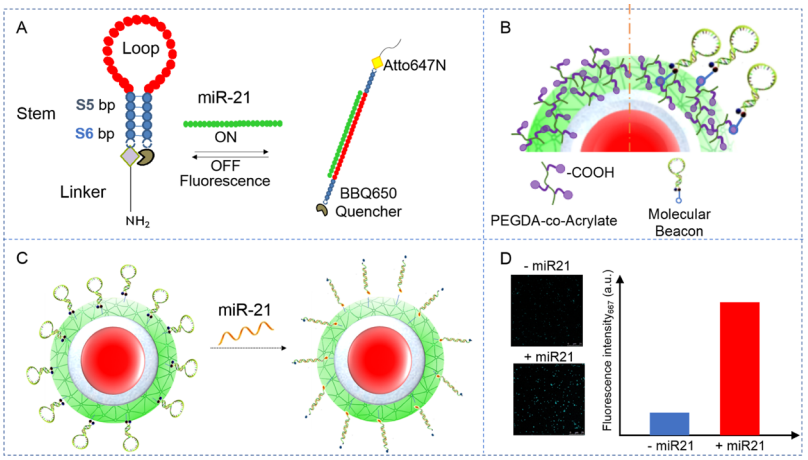

Figure 1. mbs-conjugated microgel design and mechanism of biosensing. (A) Two mb that differ from one oligonucleotide in the stem (S5−S6) have been designed for the study. In the absence of the target, the mb conforms to a stem-loop hairpin structure and fluorescence is quenched. In the presence of mir-21, fluorescence is recovered after the hybridization between the loop of the mb and the target. (B) Fluorescent microgels are endowed with carboxylic acid moieties to covalently bind the mb through their 12-carbon amino linker (5′ terminus). (C) mb-conjugated microgel are directly mixed with the sample without preliminary purification or amplification step. The circulating targets are captured by the microgels with a consequent fluorescence increment. (D) Fluorescence intensity is measured by confocal microscopy or spectrofluorometer. The target is quantified comparing the fluorescence recovery measured to a calibration curve.

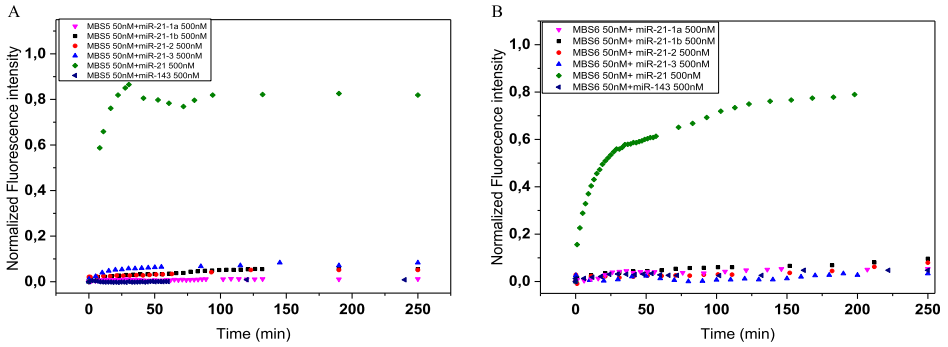

Figure 2. Hybridization kinetics of mb MBS5 (A) and MBS6 (B) in the presence of wild-type mutants miR-21 and miR-143.

loaded into the microwell and incubated at room temperature. Then, images were collected by CLSM and analyzed as previously described.

Statistical Analysis. All experiments were performed at least three times, reported as mean ± standard deviation (SD) and analyzed statistically by paired Student's test. Significant difference was determined at P values smaller than 0.05.

RESULTS AND DISCUSSION

In Figure 1 the fundamental steps involved in mb-microgels assay development are summarized: the design of the mb (Figure 1A), the bioconjugation on microgels (Figure 1B), the target recognition mechanism (Figure 1C), and the fluorescence readout (Figure 1D).

mb Design. The design of mb affects both the sensitivity and the specificity of the hybridization with the target. The main parameters considered during the mb design are the length and the sequence of the loop and the stem,[60,61] as they participate in the three different conformational states: bound to target, stem loop, and random coil. Such conformation change can be affected by bioconjugation at the microgel interface; therefore, to explore their mechanism, two mb, MBS5 and MBS6 (Table 1), are designed and tested. The mb share a common loop (22 nt) complementary to the miR-21 and a stem of 5 (MBS5) or 6 (MBS6) bases. For their design, specific software programs are used to predict the structure and thermodynamic properties. The folding studies (Supporting Information Figure S1) do not predict secondary structures in the loop, for both sequences. Moreover, because of the high GC content, the stem possesses a high stability ($\Delta G < 0$) in assay conditions.

Mb are previously tested in solution. As expected, the mb with a shorter stem (MBS5) results in target hybridization faster as compared to the mb with a longer stem (MBS6). In particular, as shown in Figure 2A, MBS5 needs 30 min to reach the complete target hybridization, whereas MBS6 requires about 150 min in the same experimental condition (Figure 2B). Moreover, the melting temperature increases with the length of the stem varying from 72.5 °C for MBS5 to 82.5 °C for MBS6 (Supporting Information Figure S2 and Table S1).

Both mb prove enhanced specificity in target recognition in solution. In particular, the hybridization kinetics and melting curve of MBS5 and MBS6 with miR-21 containing one, two, or three modifications are analyzed. As shown in Figure 2A,B, the fluorescence increment, because of hybridization with the mutated miR, is negligible compared to the wild-type miR-21.

The melting curves confirm that with proper design, mb have the potential to distinguish single-base variations in the target miRNA. Indeed, the melting temperature of the miR-mb duplex decreases as the number of point mutations increases (Supporting Information Figure S2 and Table S1).

DOI: 10.1021/acsami.8b22635
ACS Appl. Mater. Interfaces 2019, 11, 17147−17156

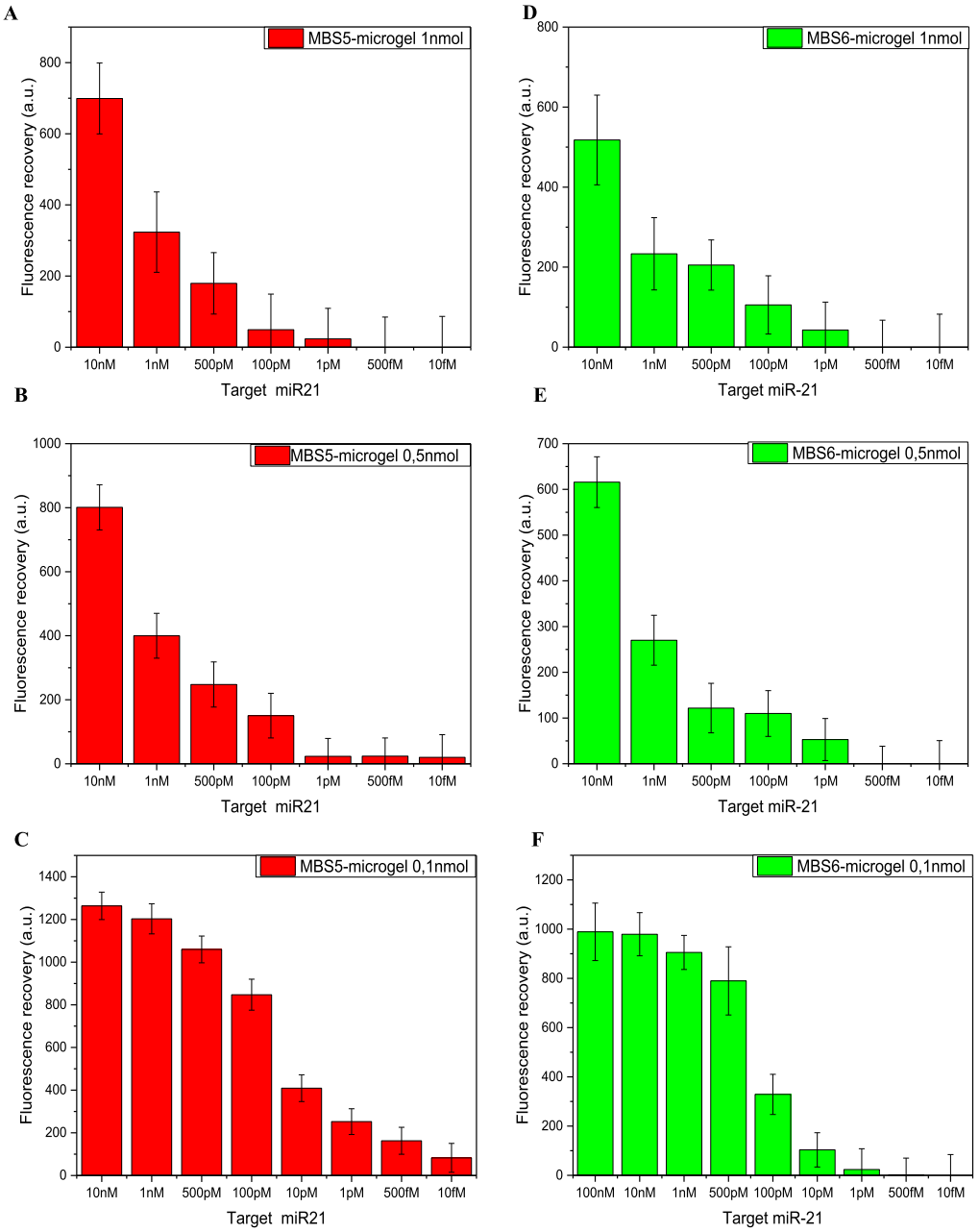

Figure 3. Microgel assay performance. Microgels are functionalized with MBS5 (red) or MBS6 (green) coupling 1 nmol (A–D), 0.5 nmol (B–E), and 0.1 nmol (C–F) of mb and put in contact with the target (nM to fM).

Microgel Synthesis and Bioconjugation. Microgels have a core with a hydrodynamic diameter (D_h) of 416.2 ± 0.9 nm. After the addition of the first shell, it grows up to 889.4 ± 18.05 nm, reaching the final diameter of 1002 ± 16.3 nm after the second shell addition (Supporting Information Table S2). The particle mass increases after each polymerization step (see Supporting Information Table S4). About 1.41×10^{10} microgels for mg are obtained via the described multistep reactions. The outer shell of microgels is enriched with carboxyl moieties to immobilize amino probes, and the amount of carboxyl group for 1 mg of microgels is 1.71 μmoles (as described in Supporting Information Figure S5). Additionally, the carboxyl groups confer to microgels the pH-responsive swelling property. Indeed, under the same ionic strength, increasing the degree of deprotonation of carboxylic acid increases the microgel size (Supporting Information Figure S3) because of the reduction of hydrogen bonding between carboxylic acid and the increase of electrostatic repulsions between anionic carboxylate groups. On the contrary, microgels are stable in a high-ionic-strength environment (Supporting Information Table S3) and show colloidal properties and enhanced stability over the time. The mesh size of the outer layer of the microgel (2nd shell) is about 4 nm.[46]

In order to set the optimal spatial distribution of mb at the interface, different bioconjugation conditions are carried out. Before the carbodiimide coupling, mb are pre-hybridized in an MES buffer with higher ionic strength. The high ionic strength helps mb to conform to their quenched hairpin structure during the immobilization step in an acid MES buffer. This step avoids non-structured mb to be conjugated within the layer with reduced mesh size, where they can be hindered to

DOI: 10.1021/acsami.8b22635
ACS Appl. Mater. Interfaces 2019, 11, 17147–17156

Table 2. mb-Microgel Assay Sensitivity

	molecular beacon functionalization					
	1 nmol		0.5 nmol		0.1 nmol	
	LOD	LOQ	LOD	LOQ	LOD	LOQ
MBS5-microgels (5 μg/mL)	71.2 pM	215.8 pM	4.5 pM	13.8 pM	105.7 fM	320.5 fM
MBS6-microgels (5 μg/mL)	443.8 pM	1.34 nM	185.8 pM	542.4 pM	324.8 fM	984.3 fM
MBS5-microgels (0.5 μg/mL)			11.9 fM	36.2 fM		
MBS6-microgels (0.5 μg/mL)			14.1 fM	42.9 fM		

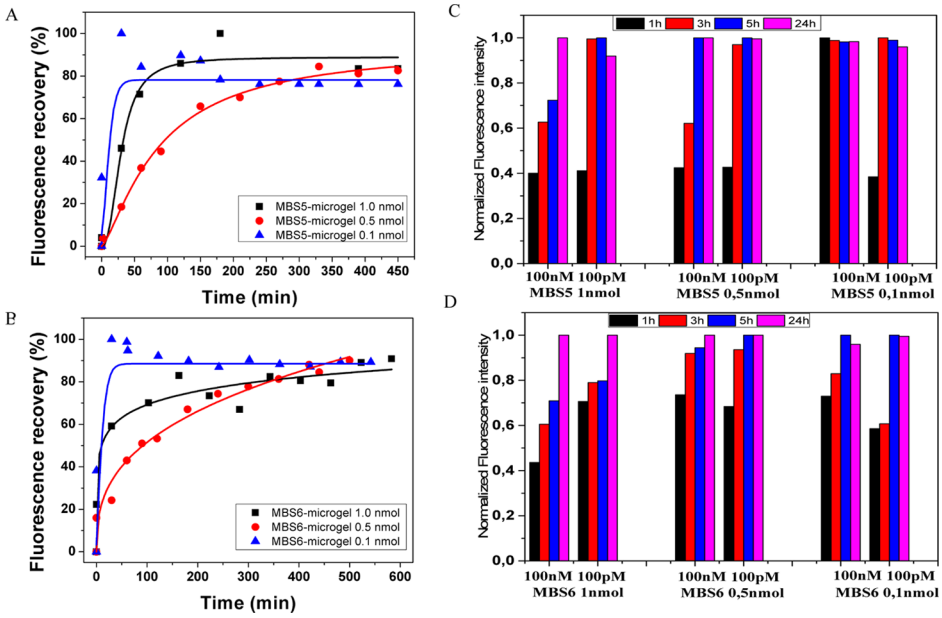

Figure 4. Hybridization kinetics measured by spectrofluorometer for MBS5 and MBS6 by spectrofluorometer (A,B) and confocal microscope (C,D).

conform to their hairpin structure, thus increasing the fluorescence background.

From the analysis of bioconjugation results, both the signal-to-noise ratio and the assay sensitivity are affected, increasing the number of mb coupled to the microgel. In particular, the signal-to-noise ratio increased about twice, reducing the functionalization from 1 to 0.1 nmol for both mb (1.78- and 1.6-fold for MBS5 and MBS6, respectively).

These results are consistent with other studies and are especially associated with the crowding effect between mb.[62,63] Indeed, the immobilization efficiency linearly increases, increasing the number of probes. However, at higher density of functionalization, the fluorescence background increases[64] and hybridization with the target is reduced because of conformational limitations imposed by the proximity of mb stem loop or by miR-mb duplexes. Therefore, decreasing the mb density, such constraint is limited, whereas the signal-to-noise ratio increases. In particular, we have found that the signal-to-noise ratio and consequently the sensitivity are remarkably improved with functionalization of 0.1 nmol, corresponding to about 4270 mb for microgel or, in the case of the outer microgel layer, about 27 000 mb for μm^3.

Assay Sensitivity and Kinetics. The mb-microgels are analyzed to define their sensitivity and kinetics of hybridizations. The results obtained (Figure 3) testing a wide range of target miR-21 clearly show that the working range is comprised between nM and fM target concentration. The assay sensitivity increases, decreasing both the length of the mb stem and the functionalization ratio. The LOD is defined as the smallest amount target or analyte that can be reliably distinguished from the background, whereas the LOQ is the smallest concentration at which not only the target can be reliably distinguished from the background but also some predefined goals for bias and imprecision are met.[65] The LOD and LOQ have been calculated, respectively, as 3.3 times the SD above the slope and 10 times the SD above the slope (Supporting Information Figure S6 and Table S5). From the analysis results, microgels functionalized with MBS5 (1, 0.5, and 0.1 nmol) reach, respectively, 71.21 pM, 4.58 pM, and 105.77 fM of LOD and 215 pM, 13.89 pM, and 320.5 fM of LOQ. Microgels functionalized with MBS6, instead, achieve 443.85 pM, 185.8 pM, and 324.8 fM of LOD and 1.34 nM, 542.4 pM and 984 fM of LOQ, conjugating with mb, respectively, at 1, 0.5, and 0.1 nmol (Table 2).

Furthermore, mb-microgel assay shows a scalable sensitivity. Indeed, by decreasing the concentration of microgels from 5 to 0.5 μg/mL per assay, the LOD further decreases (Supporting Information Figure S7). Each single microgel shows a typical dose−response curve with the highest signal-to-noise ratio corresponding to the highest level of target capture. Therefore, at a fixed amount of target, a lower number of microgels show high sensitivity because each approaches its saturation point more (highest level of target capture).[44] As a result, at a fixed amount of target, the sensitivity improves by reducing the number of microgels. In particular, MBS5 microgels reach an LOD of 11.97 fM and LOQ of 36.27 fM, whereas MBS6

DOI: 10.1021/acsami.8b22635
ACS Appl. Mater. Interfaces 2019, 11, 17147−17156

microgels reach 14.16 fM of LOD and 42.9 fM of LOQ (Supporting Information Figure S8 and Table S6).

Established that the lowest functionalization is the most performing in terms of sensitivity, we have explored the kinetic of hybridizations characteristic of each coupling by spectrofluorometer and confocal microscope. Kinetics of hybridizations—obtained by spectrofluorometer—confirms that, by decreasing the functionalization, the hybridization time decreases. In particular, MBS5 and MBS6 microgels are able to recognize the target in less than 1 h, when 0.1 nmol functionalized microgels are measured (Figure 4A,B). By increasing the functionalization degree, the kinetics of hybridization slows down. However, all microgels types tested (0.5 and 1 nmol) reach the plateau region in about 5 h. The kinetics of hybridizations are also measured by confocal microscopy, decreasing the microgel concentration from 50 to 5 μg/mL for assay. Measurements on microgels show that MBS5 microgels with higher functionalization need more than 5 h to completely hybridize with the target miR-21. Decreasing the functionalization to 0.5 nmol, the process is completed in 5 h. However, the most interesting performances are obtained by the microgels with a lower functionalization degree. Indeed, mb-microgels reach complete hybridization in 1−3 h even at a low target concentration (Figure 4C). Microgels conjugated to MBS6, compared to those functionalized with MBS5, show slower kinetics of hybridization as observed in solution. However, the microgels with lower functionalization (0.5 and 0.1 nmol) reach the complete target hybridization in a maximum of 5 h (Figure 4D).

The mb conjugation on solid surfaces arises issues in preserving a proper recognition mechanism. For this reason, mb-functionalized surfaces have not found many applications in clinical routines. The performances demonstrated in this study are mostly ascribable to PEG hydrogel molecular flexibility and conformation in water. The capability of swell and retain large volume of water generates a solution-like environment, which improves the affinity and specificity of mb. As result, by reducing the probe concentration at the interface, only the outer part of the microgel is functionalized. In such a condition, the kinetics of hybridization is not delayed and the assay time is not retarded by the diffusion, differently to what occurs in a three-dimensional or thick network, such as in the case of gel pad.[36] Moreover, mb are endowed with a long 12-carbon spacer to further reduce the steric interactions with the polymeric surface.

Compared to other mb-functionalized surfaces, the microgels allow combining advantages of mb in solution, as the faster kinetics of hybridization, with those of immobilized surfaces, as the improved sensitivity. The mb-microgels technology overcomes the limitations of current microRNA assays, such as the complicated primer design, the manipulation of the sample, and complex results read-out. Few studies have investigated the potential of combined microgel-mb systems, but, until now, this is the first technology capable at the same time to detect microRNA with high sensitivity without oligonucleotide amplification, to allow for multiplex assay by dye polymerization and to perform a direct in-serum detection. Previous studies carried out in our laboratories have already demonstrated the enhanced sensitivity of microgel-based biosensors; however, mb-microgels have also significantly improved the time of hybridization, keeping the same level of sensitivity.[40,41,44]

Assay specificity. The capacity to discriminate between oligonucleotide sequences with a single or multiple mutation is a fundamental requirement involved in developing an analytical assay. Microgels functionalized with MBS5 and MBS6 have enhanced properties in specific target recognition. Microgel specificity, indeed, is tested in the presence of non-matching sequence (miR-143-3p) and miR-21 mutants. As shown in Figure 5, MBS5 microgels are very stable toward non-matching sequences. A considerable fluorescence increment is measured only after hybridization with the wild-type target. MBS5 microgels show a slight increase in fluorescence only in the presence of mir-21-1a and mir-21-b. Such increase corresponded to the 13.1 and 14.3% of the maximum fluorescence measured after hybridization with the wild-type miR-21 at an equivalent concentration (Figure 5A). MBS6 microgels, instead, show higher specificity, and any fluorescence increment is measured when they are mixed with mir-21-1a and mir-21-b (Figure 5B). Both mb-microgels are stable

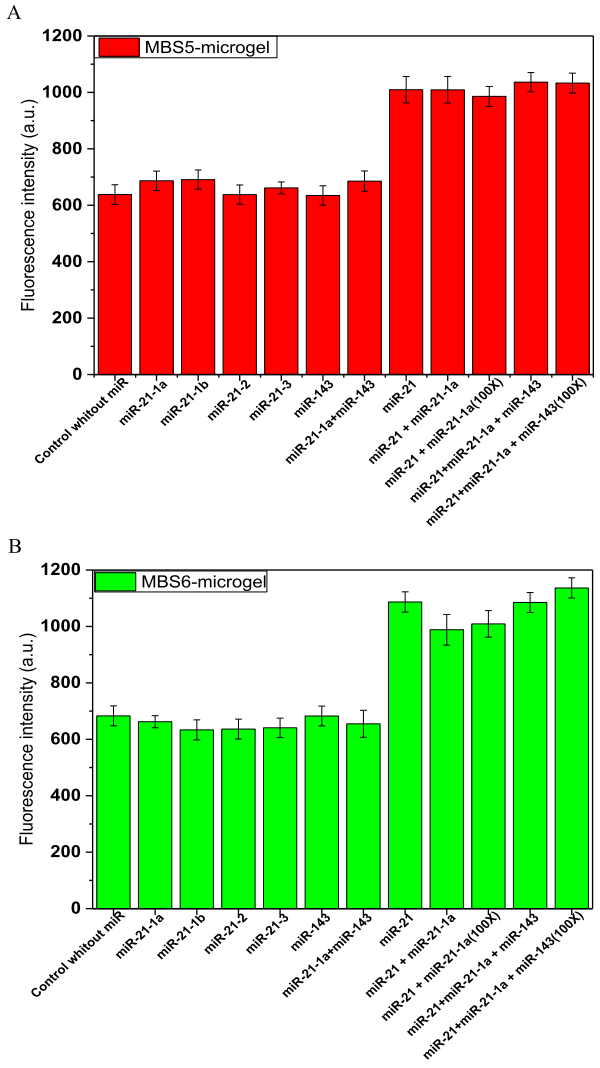

Figure 5. Specificity assay. MBS5-(A) and MBS6-(B) microgels (0.1 nmol functionalization) were tested toward wild-type miR-21, four mutated miR-21 sequences, and a non-matching sequence (miR-143). Moreover, combinations of miR-21-1a and miR143 were also tested in the absence of the wild-type target or mixed with it. In the last case, higher concentrations of miR-21-1a and miR143 were also used (5 nM-100×).

DOI: 10.1021/acsami.8b22635
ACS Appl. Mater. Interfaces 2019, 11, 17147−17156

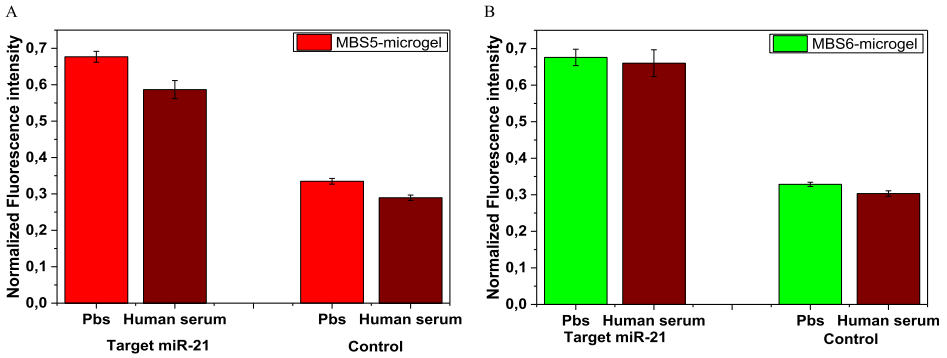

Figure 6. MBS5-microgel (A) and MBS6-microgel (B) performance in human serum and hybridization buffer (PBS), in the presence of 2 pmol of miRNA target. Fluorescence ATTO647N intensity is normalized to the rhodamine intensity.

in the presence of the mixture of miRNAs, as miR-21-1a and miR-143. Moreover, when these sequences are added to the wild-type target, they do not interfere with the recognition. As a result, the same increase in fluorescence intensity is measured both when miR-21-1a is alone and when it is combined with miR-143 added 1:1(50 pM) or 1:100(5 nM) to the wild-type miR-21. These results confirm that mb-microgels retain the mb capability of SNP sensitivity because of an appropriate development of the mb-microgel interface.

Assay in Complex Fluids. In order to simulate a real human sample, MBS5 and MBS6 microgels have been added to a small volume of human serum, enriched with 2 pmol of target and tested without prior manipulation. Both MB microgels are capable of detecting the wild-type target in human serum, with results analogous to those obtained in hybridization buffer (Figure 6A,B). Indeed, because of the antifouling nature of PEG, interfering proteins circulating in body fluids are rejected from the surface of microgels, minimizing nonspecific interactions and improving the hybridization with the target. This result highlights the enhanced efficiency of such microgels as mix&read biosensors, which represent an innovative and interesting field in biosensing.

CONCLUSIONS

Mb-microgel represents an efficient biosensor for optical detection of miR-21. In this work, we developed a new interface by engineering supramolecular PEG hydrogels with mb. Such interface offered by the microgel is innovative over other polymeric microparticles for their antifouling properties (allowing direct and specific detection without any surface treatment) and for core−shell architecture (permitting stable and high multiplex ability).

Moreover, by considering the particle nature of the hydrogel, the fluorescence—generated after target recognition—is confined to the small volume of a single microgel. This allows detecting miR-21 with scalable sensitivity down to the fM range. The assay requires only 20 μL of sample and it is completed, in worse conditions, in 3 h, avoiding preliminary amplification steps. We have also proved that mb-microgels are characterized by high specificity because they can distinguish the wild-type target from a microRNA with a single nucleotide mismatch. Furthermore, the antifouling property of the PEG microgel allows for direct use in biological fluids without the use of any surface treatment. Here we have demonstrated that the presence of human serum does not affect the sensing performance, allowing for a direct detection.

The interest in the microRNAs field is growing; however, clinical applications are still limited also because of the difficulties in their detection methods. Many efforts have been made; however, current tests suffer from important limitations, such as cost, time of analysis, and the complexity in specific probe design as there are technical difficulties in result interpretation. The mb-microgels presented in this study are specifically developed for miR-21 detection; however, the current work paves the way to a new class of microgels-based biosensors capable of sensitive detection of several microRNAs in human fluids. In this perspective, the microgel core−shell microstructure represents an approach to obtain a wide range of barcodes for multiplex purpose. Indeed, by changing the relative amount of dyes in each compartment, we can develop a variety of different optically encoded microgels. Here, we have shown a single couple of dyes, but many others can be easily copolymerized within the microgel polymeric network. Furthermore, such innovative interface between polymer hydrogel and mb could be extended to other probes, such as hairpin, aptamers, or PNA. Such promising results open new routes in biosensing for the application of mb-microgels as a biosensor capable of detecting circulating biomarker in human fluids with outstanding analytical capability moving toward noninvasive, sensitive, and portable bioanalytical devices.

ASSOCIATED CONTENT

Supporting Information

The Supporting Information is available free of charge on the ACS Publications website at DOI: 10.1021/acsami.8b22635.

Folding simulation, melting curves, T_m of mbs MBS5 and MBS6, microgel size, zeta potential, electrophoretic mobility, and conductivity measurements, microgel characterization as a function of pH and salt, microgel viscosimetry measurements, mass determination, and carboxyl acid titration, fluorescence intensity as a function of the target used to calculate the LOD and LOQ of mb-microgels (5 μg/mL), working range determination, and fluorescence intensity as a function of the target used to calculate the LOD and LOQ of mb-microgel (0.5 μg/mL) (PDF)

AUTHOR INFORMATION

Corresponding Author

*E-mail: causa@unina.it.

ORCID

Edmondo Battista: 0000-0003-0915-9176

DOI: 10.1021/acsami.8b22635
ACS Appl. Mater. Interfaces 2019, 11, 17147−17156

Filippo Causa: 0000-0002-5436-3857

Funding

RARE-PLAT-NET POR FESR CAMPANIA 2014/2020

Notes

The authors declare no competing financial interest.

REFERENCES

(1) Tyagi, S.; Kramer, F. R. Molecular Beacons: Probes That Fluoresce Upon Hybridization. *Nat. Biotechnol.* **1996**, *14*, 303−308.
(2) Goel, G.; Kumar, A.; Puniya, A. K.; Chen, W.; Singh, K. Molecular Beacon: A Multitask Probe. *J. Appl. Microbiol.* **2005**, *99*, 435−442.
(3) Wang, K.; Tang, Z.; Yang, C. J.; Kim, Y.; Fang, X.; Li, W.; Wu, Y.; Medley, C. D.; Cao, Z.; Li, J.; Colon, P.; Lin, H.; Tan, W.; Lin, H.; Tan, W. Molecular Engineering of DNA: Molecular Beacons. *Angew. Chem., Int. Ed.* **2009**, *48*, 856−870.
(4) Lakowicz, J. R. Quenching of Fluorescence. In *Principles of Fluorescence Spectroscopy*; Springer US: Boston, MA, 1983; pp 257−301.
(5) Tsourkas, A.; Behlke, M. A.; Rose, S. D.; Bao, G. Hybridization Kinetics and Thermodynamics of Molecular Beacons. *Nucleic Acids Res.* **2003**, *31*, 1319−1330.
(6) Marras, S. A. E.; Russell Kramer, F.; Tyagi, S. Multiplex Detection of Single-Nucleotide Variations Using Molecular Beacons. *Genet. Anal.* **1999**, *14*, 151−156.
(7) Marras, S. A. E.; Kramer, F. R.; Tyagi, S. *Genotyping SNPs with Molecular Beacons*; Springer: Totowa, New Jersey, 2003.
(8) Dubertret, B.; Calame, M.; Libchaber, A. J. Single-Mismatch Detection Using Gold-Quenched Fluorescent Oligonucleotides. *Nat. Biotechnol.* **2001**, *19*, 365−370.
(9) Kim, J. K.; Choi, K.-J.; Lee, M.; Jo, M.-h.; Kim, S. Molecular Imaging of a Cancer-Targeting Theragnostics Probe Using a Nucleolin Aptamer- and MicroRNA-221 Molecular Beacon-Conjugated Nanoparticle. *Biomaterials* **2012**, *33*, 207−217.
(10) Wang, H.-N.; Vo-Dinh, T. Multiplex Detection of Breast Cancer Biomarkers Using Plasmonic Molecular Sentinel Nanoprobes. *Nanotechnology* **2009**, *20*, 065101.
(11) Wang, C.; Zhang, H.; Zeng, D.; Sun, W.; Zhang, H.; Aldalbahi, A.; Wang, Y.; San, L.; Fan, C.; Zuo, X.; Mi, X. Elaborately designed diblock nanoprobes for simultaneous multicolor detection of microRNAs. *Nanoscale* **2015**, *7*, 15822.
(12) Guo, Q.; Bai, Z.; Liu, Y.; Sun, Q. A Molecular Beacon Microarray Based on a Quantum Dot Label for Detecting Single Nucleotide Polymorphisms. *Biosens. Bioelectron.* **2016**, *77*, 107−110.
(13) Horejsh, D.; Martini, F.; Poccia, F.; Ippolito, G.; Di Caro, A.; Capobianchi, M. R. A Molecular Beacon, Bead-Based Assay for the Detection of Nucleic Acids by Flow Cytometry. *Nucleic Acids Res.* **2005**, *33*, No. e13.
(14) Yao, G.; Tan, W. Molecular-Beacon-Based Array for Sensitive DNA Analysis. *Anal. Biochem.* **2004**, *331*, 216−223.
(15) Du, H.; Disney, M. D.; Miller, B. L.; Krauss, T. D. Hybridization-Based Unquenching of DNA Hairpins on Au Surfaces: Prototypical "Molecular Beacon−" Biosensors. *J. Am. Chem. Soc.* **2003**, *125*, 4012−4013.
(16) Nakano, S.-i.; Miyoshi, D.; Sugimoto, N. Effects of Molecular Crowding on the Structures, Interactions, and Functions of Nucleic acids. *Chem. Rev.* **2014**, *114*, 2733−2758.
(17) Liu, H.; Wang, H.; Shi, Z.; Wang, H.; Yang, C.; Silke, S.; Tan, W.; Lu, Z. TaqMan Probe Array for Quantitative Detection of DNA Targets. *Nucleic Acids Res.* **2006**, *34*, No. e4.
(18) Wang, H.; Li, J.; Liu, H.; Liu, Q.; Mei, Q.; Wang, Y.; Zhu, J.; He, N.; Lu, Z. Label-Free Hybridization Detection of a Single Nucleotide Mismatch by Immobilization of Molecular Beacons on an Agarose Film. *Nucleic Acids Res.* **2002**, *30*, No. e61.
(19) Wang, L.; Yang, C. J.; Medley, C. D.; Benner, S. A.; Tan, W. Locked Nucleic Acid Molecular Beacons. *J. Am. Chem. Soc.* **2005**, *127*, 15664−15665.
(20) Xu, Q.; Lou, X.; Wang, L.; Ding, X.; Yu, H.; Xiao, Y. Rapid, Surfactant-Free, and Quantitative Functionalization of Gold Nanoparticles with Thiolated DNA under Physiological PH and Its Application in Molecular Beacon-Based Biosensor. *ACS Appl. Mater. Interfaces* **2016**, *8*, 27298−27304.
(21) Yin, H.; Zhou, Y.; Zhang, H.; Meng, X.; Ai, S. Electrochemical Determination of MicroRNA-21 Based on Graphene, LNA Integrated Molecular Beacon, AuNPs and Biotin Multifunctional Bio Bar Codes and Enzymatic Assay System. *Biosens. Bioelectron.* **2012**, *33*, 247−253.
(22) Darbandi, A.; Datta, D.; Patel, K.; Lin, G.; Stroscio, M. A.; Dutta, M. Molecular Beacon Anchored onto a Graphene Oxide Substrate. *Nanotechnology* **2017**, *28*, 375501.
(23) Li, F.; Huang, Y.; Yang, Q.; Zhong, Z.; Li, D.; Wang, L.; Song, S.; Fan, C. A Graphene-Enhanced Molecular Beacon for Homogeneous DNA Detection. *Nanoscale* **2010**, *2*, 1021−1026.
(24) Oh, H. J.; Kim, J.; Park, H.; Chung, S.; Hwang, D. W.; Lee, D. S. Graphene-oxide quenching-based molecular beacon imaging of exosome-mediated transfer of neurogenic miR-193a on microfluidic platform. *Biosens. Bioelectron.* **2019**, *126*, 647.
(25) Cui, L.; Lin, X.; Lin, N.; Song, Y.; Zhu, Z.; Chen, X.; Yang, C. J. Graphene Oxide-Protected DNA Probes for Multiplex MicroRNA Analysis in Complex Biological Samples Based on a Cyclic Enzymatic Amplification Method. *Chem. Commun.* **2012**, *48*, 194−196.
(26) Chan, V.; Graves, D. J.; McKenzie, S. E. The Biophysics of DNA Hybridization with Immobilized Oligonucleotide Probes. *Biophys. J.* **1995**, *69*, 2243−2255.
(27) Steemers, F. J.; Ferguson, J. A.; Walt, D. R. Screening Unlabeled DNA Targets with Randomly Ordered Fiber-Optic Gene Arrays. *Nat. Biotechnol.* **2000**, *18*, 91−94.
(28) Ahmed, E. M. Hydrogel: Preparation, Characterization, and Applications: A Review. *J. Adv. Res.* **2015**, *6*, 105−121.
(29) Peppas, N.; Bures, P.; Leobandung, W.; Ichikawa, H. Hydrogels in Pharmaceutical Formulations. *Eur. J. Pharm. Biopharm.* **2000**, *50*, 27−46.
(30) Peppas, N. A.; Van Blarcom, D. S. Hydrogel-Based Biosensors and Sensing Devices for Drug Delivery. *J. Controlled Release* **2016**, *240*, 142−150.
(31) Le Goff, G. C.; Srinivas, R. L.; Hill, W. A.; Doyle, P. S. Hydrogel Microparticles for Biosensing. *Eur. Polym. J.* **2015**, *72*, 386−412.
(32) Choi, W.; Yeom, S. Y.; Kim, J.; Jung, S.; Jung, S.; Shim, T. S.; Kim, S. K.; Kang, J. Y.; Lee, S. H.; Cho, I.-J.; Choi, J.; Choi, N. Hydrogel micropost-based qPCR for multiplex detection of miRNAs associated with Alzheimer's disease. *Biosens. Bioelectron.* **2018**, *101*, 235−244.
(33) Liu, Y.; Wu, H.; Zhou, Q.; Song, Q.; Rui, J.; Zou, B.; Zhou, G. Digital Quantification of Gene Methylation in Stool DNA by Emulsion-PCR Coupled with Hydrogel Immobilized Bead-Array. *Biosens. Bioelectron.* **2017**, *92*, 596−601.
(34) Ma, Y.; Dai, X.; Hong, T.; Munk, G. B.; Libera, M. A NASBA on Microgel-Tethered Molecular-Beacon Microarray for Real-Time Microbial Molecular Diagnostics. *Analyst* **2017**, *142*, 147−155.
(35) Al-Ameen, M. A.; Ghosh, G. Sensitive Quantification of Vascular Endothelial Growth Factor (VEGF) Using Porosity Induced Hydrogel Microspheres. *Biosens. Bioelectron.* **2013**, *49*, 105−110.
(36) Sorokin, N. V.; Chechetkin, V. R.; Pan'kov, S. V.; Somova, O. G.; Livshits, M. A.; Donnikov, M. Y.; Turygin, A. Y.; Barsky, V. E.; Zasedatelev, A. S. Kinetics of Hybridization on Surface Oligonucleotide Microchips: Theory, Experiment, and Comparison with Hybridization on Gel-Based Microchips. *J. Biomol. Struct. Dyn.* **2006**, *24*, 57−66.
(37) Goyette, J.; Salas, C. S.; Coker-Gordon, N.; Bridge, M.; Isaacson, S. A.; Allard, J.; Dushek, O. Biophysical Assay for Tethered Signaling Reactions Reveals Tether-Controlled Activity for the Phosphatase SHP-1. *Sci. Adv.* **2017**, *3*, No. e1601692.
(38) Battista, E.; Causa, F.; Netti, P. Bioengineering Microgels and Hydrogel Microparticles for Sensing Biomolecular Targets. *Gels* **2017**, *3*, 20.

DOI: 10.1021/acsami.8b22635
ACS Appl. Mater. Interfaces 2019, 11, 17147−17156

(39) Dai, X.; Yang, W.; Firlar, E.; Marras, S. A. E.; Libera, M. Surface-Patterned Microgel-Tethered Molecular Beacons. *Soft Matter* **2012**, *8*, 3067.
(40) Causa, F.; Aliberti, A.; Cusano, A. M.; Battista, E.; Netti, P. A. Supramolecular Spectrally Encoded Microgels with Double Strand Probes for Absolute and Direct MiRNA Fluorescence Detection at High Sensitivity. *J. Am. Chem. Soc.* **2015**, *137*, 1758−1761.
(41) Aliberti, A.; Cusano, A. M.; Battista, E.; Causa, F.; Netti, P. A. High Sensitive and Direct Fluorescence Detection of Single Viral DNA Sequences by Integration of Double Strand Probes onto Microgels Particles. *Analyst* **2016**, *141*, 1250−1256.
(42) Pregibon, D. C.; Doyle, P. S. Optimization of Encoded Hydrogel Particles for Nucleic Acid Quantification. *Anal. Chem.* **2009**, *81*, 4873−4881.
(43) Kim, J. J.; Chen, L.; Doyle, P. S. Microparticle Parking and Isolation for Highly Sensitive MicroRNA Detection. *Lab Chip* **2017**, *17*, 3120−3128.
(44) Caputo, T. M.; Cummaro, A.; Lettera, V.; Mazzarotta, A.; Battista, E.; Netti, P. A.; Causa, F. One-Step Scalable Fluorescent Microgel Bioassay for Endogenous Viral MiR-US4-5p Ultrasensitive Detection. *Analyst* **2018**, *144*, 1369−1378.
(45) Pregibon, D. C.; Toner, M.; Doyle, P. S. Multifunctional Encoded Particles for High-Throughput Biomolecule Analysis. *Science* **2007**, *315*, 1393−1396.
(46) Battista, E.; Mazzarotta, A.; Causa, F.; Cusano, A. M.; Netti, P. A. Core−shell microgels with controlled structural properties. *Polym. Int.* **2016**, *65*, 747−755.
(47) Choi, N. W.; Kim, J.; Chapin, S. C.; Duong, T.; Donohue, E.; Pandey, P.; Broom, W.; Hill, W. A.; Doyle, P. S. Multiplexed Detection of MRNA Using Porosity-Tuned Hydrogel Microparticles. *Anal. Chem.* **2012**, *84*, 9370−9378.
(48) Dannhauser, D.; Causa, F.; Battista, E.; Cusano, A. M.; Rossi, D.; Netti, P. A. In-Flow Real-Time Detection of Spectrally Encoded Microgels for MiRNA Absolute Quantification. *Biomicrofluidics* **2016**, *10*, 064114.
(49) Tackett, M.; Doran, G.; Pregibon, D. Multiplex MicroRNA Profiling from Crude Biofluids. *Genet. Eng. Biotechnol. News* **2015**, *35*, 14−15.
(50) Bartel, D. P. MicroRNAs. *Cell* **2004**, *116*, 281−297.
(51) Peng, Y.; Croce, C. M. The Role of MicroRNAs in Human Cancer. *Signal Transduction Targeted Ther.* **2016**, *1*, 15004.
(52) Xu, J.; Zhao, J.; Evan, G.; Xiao, C.; Cheng, Y.; Xiao, J. Circulating MicroRNAs: Novel Biomarkers for Cardiovascular Diseases. *J. Mol. Med.* **2012**, *90*, 865−875.
(53) Quinlan, S.; Kenny, A.; Medina, M.; Engel, T.; Jimenez-Mateos, E. M. MicroRNAs in Neurodegenerative Diseases. *Int. Rev. Cell Mol. Biol.* **2017**, *334*, 309−343.
(54) Louten, J.; Beach, M.; Palermino, K.; Weeks, M.; Holenstein, G. MicroRNAs Expressed during Viral Infection: Biomarker Potential and Therapeutic Considerations. *Biomark. Insights* **2016**, *10*, 25−52.
(55) Hunt, E. A.; Broyles, D.; Head, T.; Deo, S. K. MicroRNA Detection: Current Technology and Research Strategies. *Annu. Rev. Anal. Chem.* **2015**, *8*, 217−237.
(56) Tian, T.; Wang, J.; Zhou, X. A Review: MicroRNA Detection Methods. *Org. Biomol. Chem.* **2015**, *13*, 2226−2238.
(57) De Planell-Saguer, M.; Rodicio, M. C. Detection Methods for MicroRNAs in Clinic Practice. *Clin. Biochem.* **2013**, *46*, 869−878.
(58) Kumarswamy, R.; Volkmann, I.; Thum, T. Regulation and Function of MiRNA-21 in Health and Disease. *RNA Biol.* **2011**, *8*, 706−713.
(59) Krichevsky, A. M.; Gabriely, G. miR-21: a small multi-faceted RNA. *J. Cell Mol. Med.* **2009**, *13*, 39−53.
(60) Zheng, J.; Yang, R.; Shi, M.; Wu, C.; Fang, X.; Li, Y.; Li, J.; Tan, W. Rationally Designed Molecular Beacons for Bioanalytical and Biomedical Applications. *Chem. Soc. Rev.* **2015**, *44*, 3036−3055.
(61) Marras, S. A. E. Selection of Fluorophore and Quencher Pairs for Fluorescent Nucleic Acid Hybridization Probes. In *Fluorescent Energy Transfer Nucleic Acid Probes*; Methods in Molecular Biology; Humana Press: New Jersey, 2006; Vol. 335, pp 3−16.
(62) Peterson, A. W.; Heaton, R. J.; Georgiadis, R. M. The Effect of Surface Probe Density on DNA Hybridization. *Nucleic Acids Res.* **2001**, *29*, 5163−5168.
(63) Traeger, J. C.; Schwartz, D. K. Surface-Mediated DNA Hybridization: Effects of DNA Conformation, Surface Chemistry, and Electrostatics. *Langmuir* **2017**, *33*, 12651−12659.
(64) Ma, Y.; Libera, M. Molecular Crowding Effects on Microgel-Tethered Oligonucleotide Probes. *Langmuir* **2016**, *32*, 6551−6558.
(65) Armbruster, D. A.; Pry, T. Limit of blank, limit of detection and limit of quantitation. *Clin. Biochem. Rev.* **2008**, *29*, S49−S52.

DOI: 10.1021/acsami.8b22635
ACS Appl. Mater. Interfaces 2019, 11, 17147−17156